C.A9350057

TRI-PP-88-33
May 1988

Ratio of Spin Transfer Parameters d_t/r_t in $d(\vec{p},\vec{n})pp$ Quasi-Elastic Scattering

R. Abegg[1], D. Bandyopadhyay[2], J. Birchall[2], C. A. Davis[2], N. E. Davison[2], P. W. Green[1], L. G. Greeniaus[1,3], C. Lapointe[3], C. A. Miller [1], G. A. Moss [3], S. A. Page[2], W. D. Ramsay[2], R. R. Tkachuk[3], and W. T. H. van Oers[2]

(1) TRIUMF, 4004 Wesbrook Mall, Vancouver, B. C., V6T 2A3, Canada.
(2) Department of Physics, University of Manitoba, Winnipeg, Manitoba, R3T 2N2, Canada.
(3) Department of Physics, University of Alberta, Edmonton, Alberta, T6G 2N5, Canada.

ABSTRACT

The ratio of spin transfer parameters d_t/r_t for the quasi-elastic process $d(\vec{p},\vec{n})pp$ has been measured at four energies between 200 and 500 MeV at a neutron scattering angle of 9 degrees. From this, the following values of D_t/R_t for free np scattering have been deduced: -0.0190 ± 0.0072 (T_p = 223 MeV); -0.2328 ± 0.0057 (324 MeV); -0.3731 ± 0.0068 (425 MeV); -0.4892 ± 0.0107 (492 MeV). These values have a noticeable effect on present day phase shift solutions. The magnitude of the ϵ_1 mixing parameter is reduced and other phase shifts are smoother around 300 MeV.

(submitted to Physical Review C)

I. INTRODUCTION

The nucleon-nucleon interaction is fundamental to the understanding of both nuclear and particle physics. It has been extensively studied over a wide range of angles and energies for many observables of the two nucleon system. These results have been used to generate values for the phase shifts that parametrize the scattering matrix.[1,2,3] Even though the phase shift fits appear to be quite stable up to 800 MeV for proton-proton scattering and up to 650 MeV for neutron-proton scattering, the fact that the χ^2 per datum is significantly greater than one indicates that problems, possibly in the data base, need to be resolved. The two modern nucleon-nucleon potentials, the "Paris"[4] and "Bonn"[5] potentials, provide predictions for the nucleon-nucleon observables and phase shifts which in some cases are very different. These discrepancies need to be investigated through experiments more sensitive to the phase shifts in question. Despite the great number of previous np measurements, the present experiment provides important constraints on the phase shifts because of its sensitivity to a few phase shifts, its high accuracy, and because it provides information where previous data are sparse.[6]

The ratio d_t/r_t in $d(\vec{p},\vec{n})pp$ quasi-elastic scattering was determined at incident proton energies: T_p = 223, 324, 425, and 492 MeV at a neutron laboratory angle of 9 degrees (about 160 degrees c. m.). D_t is the vertical to vertical transverse spin transfer parameter (D_{nn} or K_{onno}) and R_t is the horizontal to horizontal transverse spin transfer parameter (K_{ss} or K_{osso}) in free np scattering. The quantities d_t and r_t are their equivalents for the quasi-elastic scattering from deuterium. Measurement of a ratio eliminates many sources of systematic error associated with the determination of the incoming proton and outgoing neutron polarizations. The observed values of d_t/r_t have statistical accuracies ranging from 0.0045 to 0.0085 and systematic errors ranging from 0.0032 to 0.0060. Using calculations of Bugg and Wilkin[7] to compensate for the effects of final state interactions and the deuteron D-state, values for the ratio D_t/R_t for free np scattering were deduced with very little error from the theoretically based correction.

In Section II, a brief description is given of the experimental apparatus. In Section III, the data analysis is discussed, while Section IV contains a discussion of systematic errors. In Section V, the results are presented and the influence of the data on the phase shift parameters is discussed.

II. EXPERIMENTAL APPARATUS

The TRIUMF Neutron Beam Facility has been discussed extensively in ref. 8 and additional information may be found in references 9 and 10. The experimental layout of the present experiment is shown in Fig. 1.

The extracted proton beam was transferred along the TRIUMF 4A beamline where it passed through two polarimeters, the first of which was a large acceptance (2.80 msr) four-branch device[11] where the ratio of the normal and

sideways components of beam polarization (P_x/P_y) was determined with high accuracy. Protons elastically scattered at 17 degrees from the hydrogen in a 0.55 mg/cm^2 CH_2 target were detected in coincidence with the recoil protons. The second polarimeter was a small acceptance (0.16 msr) two-branch polarimeter counting protons scattered at an angle of 17 degrees in coincidence with their recoils scattered from a 3.5-4.0 mg/cm^2 Kapton target. This polarimeter measured only the normal component of polarization and allowed a determination of $P_y A_k$ with high accuracy, where A_k is the analyzing power of the Kapton target. Periodically a CH_2 target and a graphite target were substituted in the second polarimeter to investigate possible changes in the value of the effective A_k as a function of time and to determine the $^{12}C(p,2p)$ contribution to A_k. Beam polarization fluctuations were monitored by using the first proton polarimeter as a reference during these calibration runs. Both polarimeters had solid angle defining counters that were rotated to compensate for the effects of beam motion on the target.[12]

After the polarimeters, the beam passed through a super-conducting solenoid which precessed P_y into the horizontal plane (x-direction) for the R_t measurement. The solenoid was not powered for the D_t measurement. Split-plate secondary emission monitors (SEMs) were located upstream and downstream of the solenoid; their outputs were used to control two horizontal and two vertical steering elements, which stabilized the position and angle of incidence of the beam on the target. The present experiment made use of the 0.197 m long, 50.8 mm diameter, liquid deuterium (LD_2) neutron production target as the experimental target for studying the $d(\vec{p},\vec{n})pp$ reaction. After passing through the LD_2 target, the proton beam was deflected 35 degrees by a clearing magnet and transported to the 4A beam dump.

The $d(\vec{p},\vec{n})pp$ polarized neutrons from the LD_2 target passed through a corner of the clearing magnet field and then through a 3.37 m long collimator at 8.95 degrees. The acceptance was 0.26 degrees wide by 0.18 degrees high. A second collimator between the poles of the first (vertical field) spin precession magnet restricted the tails of the neutron beam. The collimation resulted in a neutron beam 76 mm wide by 52 mm high (flat-top region) at a distance of 16.9 m from the LD_2 target. The combined effect of this magnet and the clearing magnet was to precess the horizontal transverse component of polarization into the longitudinal direction for the R_t measurement. The neutrons then passed through a second (horizontal field) spin precession magnet which precessed the longitudinal component of polarization into the the normal direction for the R_t measurement (this magnet was left off during the D_t measurement).

The neutron beam impinged on a cylindrical liquid hydrogen (LH_2) target located 12.85 m from the LD_2 target. The LH_2 target was 117 mm thick along the beam axis with two spherical end caps of 149 mm radius, the cell being 149 mm in diameter about the beam axis. The target operated typically at a temperature of 20 K and a pressure of 114 kPa. The recoil protons were detected in a ± 5 degree angle range centered at the angle of maximum np backward

angle analyzing power (30.3, 36.3, 35.5 and, 34.6 degrees in the laboratory, with increasing energy). Two proton booms were used, one on each side of the beam.[9] Each boom contained three scintillators (TOF Start, ΔE, and E) to trigger the event and allow measurement of the recoil proton time-of-flight (TOF). Each boom also contained four delay line wire chambers to permit reconstruction of the particle trajectory, a brass wedge just before the E counter, and additional brass absorber behind the E counter such that protons from free np scattering were absorbed before reaching a veto scintillator.

A test run was carried out with a 469 MeV scattered proton beam extracted along the neutron beamline. The protons were obtained from pp elastic scattering on liquid hydrogen in the LD_2 target cell. Coincident pp elastic scattering events from the LH_2 target were observed in the proton booms which were placed at 90 degrees c. m. Cuts on the acceptance of one boom were sufficiently small such that even with multiple scattering all the corresponding recoils from pp elastic scattering would be seen in the other boom. Taking into account chamber inefficiencies and subtracting the contribution of the windows, approximately 96% of all events had both tracks detected. Given that some of the protons in one boom must have resulted from inelastic pp events and that some recoil protons may have been lost due to nuclear reactions, this is a reasonable efficiency for identifying elastically scattered protons from single arm events.

Downstream of the LH_2 target the neutron beam passed through a beam profile monitor which consisted of a charged particle veto counter, a converter scintillator, and two delay line wire chambers used to reconstruct the tracks of charged particles coming from the converter. Beyond this was a four-branch neutron polarimeter which detected protons from np scattering in a CH_2 target. Due to background C(n,p) events this device had a relatively low and poorly known analyzing power and was very sensitive to beam displacement. Although the instrumental asymmetry changed by 1% per mm of neutron beam displacement at $T_n = 477$ MeV, it did provide values for the ratio of sideways to normal components of neutron polarization.

The data were collected in two modes: (1) to determine the sideways to sideways spin transfer (R_t) the solenoid and vertical and horizontal field spin-precession magnets were on, and (2) to determine the normal to normal spin transfer (D_t) the solenoid and horizontal field spin-precession magnet were off. As a solenoid is weakly focusing and rotates the phase space of the beam, some retuning of the proton beam and modification of the beam position control loop parameters were needed when switching from one mode to the other. However, the split-plate SEMs ensured that the position and direction of incidence of the beam at the LD_2 target remained the same for the two measurements. Otherwise, nothing was changed from one mode to the other. Data at each energy required about one day to acquire. For both the R_t and D_t measurements, some data were taken with the LH_2 target 'empty' (some H_2 vapour being present) and with a dummy LD_2 target (a duplicate of the LD_2 target which contained no deuterium).

At each energy change the proton polarimeter targets were replaced, the proton booms were centered at the position for the maximum absolute magnitude of the np analyzing power at backward c. m. angles and the wedges and absorbers on the proton booms were changed. The spin precession magnets were adjusted to appropriate values with the aid of an NMR system in each magnet.

The spin state of the beam was cycled automatically with 3 minutes 'Up', 1 minute unpolarized, and 3 minutes 'Down'. The event rate was approximately 100 Hz. Scalers from the polarimeters were recorded every 5 seconds and neutron beam profile data with a rate of a few Hz were also written to tape.

III. ANALYSIS

Scaler data were analyzed to extract asymmetries (corrected for accidentals) for both proton polarimeters. The four-branch polarimeter permitted determination of the ratio of the horizontal and vertical components $(P_x/P_y)_p$ of polarization to an accuracy of ± 0.002 per tape. The second proton polarimeter allowed measurement of $P_y A_k$ to an accuracy of ± 0.002 for each spin state per tape. The neutron polarimeter error on $(P_x/P_y)_n$ was typically ± 0.015 per tape for the R_t data for which it is required to estimate errors due to an additional longitudinal component of polarization of the proton beam. Information was also obtained on beam current and proton boom counter singles rates.

The trajectory of the recoiling proton from np scattering in the LH_2 target was reconstructed using the delay line wire chambers on each boom. Because of the redundancy arising from the use of four chambers, each providing x and y information, better than 99% of all events had adequate trajectory information (at least three hits in x and y). This information was used to place cuts on acceptance, target reconstruction, and trajectory reconstruction chi-square. About 4-5% of events for x and y combined were rejected by the χ^2 test. The proton trajectory was also used to help determine proton TOF corrections as a function of the hit position within the large E scintillator. The TOF distribution is a convolution of the energy spread of the neutrons and the instrumental timing resolution. The tail below the proton TOF peak contains some slower charged particles from np reactions in the LH_2 target, but is primarily due to the tail of low energy neutrons from the $d(p,n)pp$ reaction[7].

A TOF signal for the neutron was generated from the cyclotron RF signal, which was timed against the trigger for each event. With a cut on the proton TOF, the effective cut-off in the neutron energy distribution tail was determined. This is important since one needs to correct for the energy cut-off dependence of the corrections to determine D_t/R_t for free np scattering from d_t/r_t for quasi-elastic scattering[7]. For the reaction $d(\vec{p},\vec{n})pp$, described by the impulse approximation with the neutron in the deuteron undergoing a charge exchange, and taking into account the deuteron D state and final state interaction of the two protons, the spin transfer parameters are found to vary strongly across the

peak of the neutron spectrum but to vary only weakly in the tail[7]. One must be careful that all the data in the peak is included in the cuts to ensure that the result will be only weakly dependent on the correction.

Background run data were analyzed to determine the contribution from the windows of the targets. The LH_2 background is relatively inconsequential, since the effective analyzing power of this target cancels in the determination of d_t/r_t. The LD_2 target background could contribute to the neutron spectrum from quasi-elastic processes in the target window.

The spin transfer parameter r_t, averaging over the two spin states to remove dependence on the instrumental asymmetry, is given by

$$\epsilon_n(r_t) = A_n \frac{\epsilon_p(r_t)}{A_k} r_t \tag{1}$$

The spin transfer parameter d_t is related to the measured asymmetries by

$$\epsilon_n^{\pm}(d_t) = A_n \frac{\frac{\epsilon_p^{\pm}(d_t)}{A_k} d_t \pm P}{1 \pm \frac{\epsilon_p^{\pm}(d_t)}{A_k} P} + \epsilon_0 \tag{2}$$

Averaging over the two spin states gives

$$\epsilon_n(d_t) = A_n \frac{\epsilon_p(d_t)}{A_k} d_t \tag{3}$$

$$+ \text{ terms of order } P^2 A_n \text{ and higher.}$$

$\epsilon_a(b)$ is the asymmetry measurement of the a (proton or neutron) polarization for the spin-transfer parameter b, ϵ_0 is the instrumental asymmetry, A_n is the analyzing power of the LH_2 target, and P is the polarization arising from the np scattering (typically -0.06 at 160 degrees over the energy range). The ratio of the spin transfer parameters, to first order, thus depends only on the measured asymmetries

$$d_t/r_t = \frac{\epsilon_n(d_t)\epsilon_p(r_t)}{\epsilon_p(d_t)\epsilon_n(r_t)} \tag{4}$$

Analysis was carried out in a consistent manner for all D_t, R_t, and background data. With all variables unchanged, save for the direction of spin at the LD_2 target, dependence on the proton polarimeter analyzing power, A_k, or the np analyzing power, A_n, cancels out in the determination of d_t/r_t, (except for small higher order corrections) as indicated in Eq. (4). The higher order corrections of order $P^2 A_n$ were made with values of P determined from the data and values of A_n from phase shift predictions.

IV. SYSTEMATIC ERRORS

Various sources of systematic error are summarized in Table I and discussed below.

A. Foil 'Burn-out'. Ideally, the proton polarimeter analyzing power, A_k, should be the same for D_t and R_t data at a given energy. The value of A_k might change with time or integrated beam current because of a change in the C:H ratio of the Kapton (H knockout, outgassing, deposition of vacuum pump oils) or because of a change in position of the Kapton target (wrinkling due to beam heating). This was monitored periodically during each run by comparing the Kapton target to a reference CH_2 target. It was found that A_k was constant, within statistics, and the variance in these runs was used as an estimate of the limits of change in the value of A_k. This is a relative error in determining d_t/r_t.

B. Magnet Spin Precession. This could affect the R_t measurement. The spin precession magnets and the proton beam clearing magnet have had their integrated field at different excitations determined to $\pm 3\%$. Fields of these magnets were monitored by NMR systems. Field settings used for the spin-precession magnets gave spin precessions within ± 1 degree of the desired values at the average neutron energy. The super-conducting solenoid current was monitored[8] to 0.2%. The total error in neutron spin precession[10] certainly does not exceed 6 degrees.

C. Extra Components of Polarization. Due to the existence of resonances in the cyclotron, which couple the Larmor spin precession frequency with the cyclotron frequency, horizontal components of polarization whose magnitude can be dependent on the machine 'tune' are present in the beam emerging from the cyclotron. They do not effect the d_t measurement, but the longitudinal component of polarization of the proton beam can contribute through $P_z a_t$ to the r_t asymmetry. The proton polarimeters measure P_x directly. The neutron polarimeter determines $P_z a_t' + P_y r_t'$. Due to the fact that the spin transfer parameters r_t', a_t' and a_t are not well known (relative errors are r_t', 20%; a_t', 5-60%; a_t, 10-60%), and due to the spin precession uncertainty, which adds a maximum uncertainty of $P_y r_t \sin(6 \text{ degrees})$ to the neutron P_x measurement, P_z of the proton is not well known. However a reasonable limit can be placed on its magnitude, which should be about the same as P_x. Limits of $\mid P_z a_t \mid$ are given in Table I.

D. Beam Motion. The beam position was stabilized[8] by the SEM loop to ± 0.2 mm. Motion of the proton beam on the LD_2 target causes motion of the neutron beam. The position and profile of the neutron beam was monitored throughout the experiment. Differences in neutron beam position between d_t and r_t runs translated to less than 0.008 degree motion at the LH_2 target. This gives rise to an uncertainty in the value of the effective np analyzing power at the LH_2 target, which is a relative error in d_t/r_t.

E. LH_2 Target Background. The LH_2 target windows contributed less than 4% of the scattered charged particles. This does not give rise to an uncertainty

in d_t/r_t since it is present in both measurements. It does produce an uncertainty in estimating the change in analyzing power with angle to establish the error due to the small beam displacement at the LH_2 target (see D above).

F. LD_2 Target Background. The LD_2 target windows and structure contributed a background of 0.2-0.5% of the total events. The values of d_t/r_t (as given in Table II) were corrected for this background, and the statistical errors also reflect the error in determining this background.

G. Energy. The proton beam energy from the cyclotron was uncertain by ± 1.5 MeV. The slope of the measured values of d_t/r_t as a function of energy was used to determine the error arising from this uncertainty in energy. The proton energy was corrected for energy loss to the center of the LD_2 target cell. The energy cut-off for the outgoing neutron (ΔT_n), which must be reasonably well known to determine the corrections needed to deduce D_t/R_t, was known to better than $\pm$ 16 MeV. This translates in to an error in the correction to the quasi-elastic np parameters to deduce the free np parameters which is presented in Table II.

V. RESULTS AND CONCLUSIONS

The measured values for the ratio d_t/r_t, corrected for the dependence on higher order terms in $P^2 A_n$ and subtracting the effect of the LD_2 target windows, with their statistical and sytematic errors, the neutron TOF equivalent energy cut-off and its error, and the deduced values for D_t/R_t for free np scattering (obtained with the corrections of ref. 7) are presented in Table II. The systematic errors have been added in quadrature. A comparison between the present data for D_t/R_t and several phase shift predictions is made in Fig. 2. These phase shift predictions[1-3] are from Arndt et al.[13], SAID solution SM87; from Bystricky, Lechanoine-Leluc and Lehar[14], solutions S260 and S500 for two different energy ranges; and from Bugg et al.[2] Note that these predictions stem from data bases that are not necessarily identical and do not include the present data.

The impact of the present data on the energy independent phase shift solutions *C200*, *C300*, *C400*, and *C500* of the phase shift analysis program SAID[13] has been investigated. The observable D_t was given values such that the value of D_t/R_t corresponded to the experimental value well within the quoted error. The data significantly reduce the phase angles of the ϵ_1 and also ϵ_3 coupling parameters and also affect the $^3S_1$, $^3D_1$, and $^3D_2$ phase shifts. The effect on the $^1P_1$ phase shift clearly indicates problems with the existing data base around 300 MeV. Using a criterion of overall smoothness with energy, the data of the present experiment definitely improve the phase shift behavior with energy. Some large correlations between certain phase shift parameters still remain: $\epsilon_1 \times \epsilon_3$ is especially large; $^3S_1 \times ^3D_1$ is also significant across the whole energy region; $^3S_1 \times ^3D_2$ and $^3D_1 \times ^3D_2$ are significant below 300 MeV; while $\epsilon_1 \times ^1P_1$, $\epsilon_1 \times ^3D_2$, and $^1P_1 \times ^3D_2$ are significant at higher energies.

The nucleon-nucleon tensor interaction is important for nuclear binding energy calculations since it provides saturation. The strength of the tensor interaction depends on the value of the mixing angle ϵ_1 in the energy region under consideration[15] and therefore on the observable D_t[16]. A better determination of ϵ_1 is of direct importance to the question of the binding energies of the three nucleon system[15]. The values of ϵ_1 obtained when the present data are included in the phase shift analyses are compared to the predictions of the "Paris" and "Bonn" potentials (see Fig. 3), which give rather different predictions for deuteron D-state probabilities. It is further to be noted that the changes in the phase shift parameters shown in Fig. 3 are corroborated when recent preliminary np spin correlation parameter data A_{yy} are included in the phase shift analysis[17]. In summary, the present work has demonstrated that precision data on selected np observables will aid significantly in better determining the nucleon-nucleon interaction.

VI. ACKNOWLEDGEMENTS

We would like to thank Prof. D. V. Bugg for suggesting this measurement and pointing out its usefulness in constraining the present phase shift parameters. We should also like to thank the staff at TRIUMF for their valuable assistance during the execution phase of this experiment. This work was supported by the Natural Sciences and Engineering Research Council of Canada.

REFERENCES

1) R. A. Arndt, R. H. Hackman and L. D. Roper, Phys. Rev. **C9**, 555 (1974); R. A. Arndt, R. H. Hackman and L. D. Roper, Phys. Rev. **C15** , 1002 (1977); R. A. Arndt, R. H. Hackman and L. D. Roper, Phys. Rev. **C15** , 1021 (1977); R. A. Arndt, L. D. Roper, R. A. Bryan, R. B. Clark, B. J. verWest and P. Signell, Phys. Rev. **D28** , 97 (1983).

2) D. V. Bugg, J. A. Edgington, C. Amsler, R. C. Brown, C. J. Oram, K. Shakarchi, N. M. Stewart, G. A. Ludgate, A. S. Clough, D. Axen, S. Jaccard, and J. Vavra, J. Phys. **G4** , 1025 (1978); D. V. Bugg, J. A. Edgington, W. R. Gibson, N. Wright, N. M. Stewart, A. S. Clough, D. Axen, G. A. Ludgate, C. J. Oram, L. P. Robertson, J. R. Richardson and C. Amsler, Phys. Rev. **C21** , 1004 (1980); and D. V. Bugg, private communication (1985).

3) J. Bystricky, C. Lechanoine-Leluc and F. Lehar, J. Physique **48** , 199 (1987).

4) M. Lacombe, B. Loiseau, J. M. Richard, R. Vinh Mau, J. Côté, P. Pirès and R. de Tourreil, Phys. Rev. **C21** , 861 (1980); W. N. Cottingham, M. Lacombe, B. Loiseau, J. M. Richard and R. Vinh Mau, Phys. Rev. **D8** , 800 (1973); R. Vinh Mau, "The Paris N-N Potential" in "Mesons in Nuclei", edited by M. Rho and D. Wilkinson (North-Holland, Amsterdam, 1979); M. Lacombe, B. Loiseau, R. Vinh Mau, J. Côté, P. Pirès and R. de Tourreil, Institut de Physique Nucléaire (Orsay) Report No. IPNO/TH 80-60 (1980); and references therein, unpublished.

5) R. Machleidt, K. Holinde and Ch. Elster, Physics Reports **149** , 1 (1987); K. Holinde and R. Machleidt, Nucl. Phys. **A256** , 479, 497 (1976); K. Kotthoff, K. Holinde, R. Machleidt and D. Schütte, Nucl. Phys. **A242** , 429 (1975); X. Bagnoud, K. Holinde and R. Machleidt, Phys. Rev. **C29** , 1792 (1984); M. M. Nagels, T. A. Rijken and J. D. de Swart, Phys. Rev. **D20** , 1633 (1979); and references therein.

6) D. V. Bugg, Comments on Nucl. and Part. Phys. **12** , 287 (1984).

7) D. V. Bugg and C. Wilkin, Nucl. Phys. **A467** , 575 (1987).

8) R. Abegg, J. Birchall, E. B. Cairns, G. H. Coombes, C. A. Davis, N. E. Davison, P. W. Green, L. G. Greeniaus, H. P. Gubler, W. P. Lee, W. J. McDonald, C. A. Miller, G. A. Moss, G. R. Plattner, P. R. Poffenberger, G. Roy, J. Soukup, J. P. Svenne, R. Tkachuk, W. T. H. van Oers and Y. P. Zhang, Nucl. Inst. and Meth. **A234** , 11 (1985).

9) R. Abegg, J. Birchall, E. B. Cairns, G. H. Coombes, C. A. Davis, N. E. Davison, P. W. Green, L. G. Greeniaus, H. P. Gubler, W. P. Lee, W. J. McDonald, C. A. Miller, G. A. Moss, G. R. Plattner, P. R. Poffenberger, G. Roy, J. Soukup, J. P. Svenne, R. Tkachuk, W. T. H. van Oers and Y. P. Zhang, Nucl. Inst. and Meth. **A234** , 20 (1985).

10) R. Abegg, D. Bandyopadhyay, J. Birchall, E. B. Cairns, G. H. Coombes, C. A. Davis, N. E. Davison, P. P. J. Delheij, P. W. Green, L. G. Greeniaus, H. P.

Gubler, D. C. Healey, C. Lapointe, W. P. Lee, W. J. McDonald, C. A. Miller, G. A. Moss, G. R. Plattner, P. R. Poffenberger, W. D. Ramsay, G. Roy, J. Soukup, J. P. Svenne, R. R. Tkachuk, W. T. H. van Oers, G. D. Wait and Y. P. Zhang, in Proceedings Sixth International Conference on Polarization Phenomena in Nuclear Physics, Osaka 1985, J. Phys. Soc. Japan, **55** , 369 (1986) Suppl.; Phys. Rev. Lett. **56** , 2571 (1986).

11) R. Abegg and R. Schubank, TRIUMF Design Note TRI-DN-87-17, (1987), unpublished.

12) L. G. Greeniaus and J. Soukup, TRIUMF Design Note TRI-DNA-81-1, (1981), unpublished.

13) R. A. Arndt, Interactive dial-in program SAID.

14) C. Lechanoine-Leluc, private communication.

15) G. S. Chulick, Ch. Elster, R. Machleidt, A. Picklesimer and R. M. Thaler, Phys. Rev. **C37** , 1549 (1988).

16) F. Pauss, L. Mathelitsch, J. Côté, M. Lacombe, B. Loiseau, R. Vinh Mau, Institut de Physique Nucléaire (Orsay) Report No. IPNO/TH 80-39 (1980), unpublished.

17) D. Bandyopadhyay, J. Birchall, K. Chantziantoniou, C. A. Davis, N. E. Davison, S. A. Page, W. D. Ramsay, W. T. H. van Oers, R. Abegg, P. P. J. Delheij, P. W. Green, L. G. Greeniaus, D. C. Healey, C. A. Miller, G. D. Wait, M. Ahmad, C. Lapointe, W. J. McDonald, G. A. Moss, N. Rodning, G. Roy, Y. Ye and J. W. Watson, Bull. Am. Phys. Soc. **32** , 1546 (1987).

FIGURE CAPTIONS

1) Schematic lay-out of the experiment. The polarized proton beam passes through two polarimeters, through a super-conducting solenoid (which is on for R_t data and off for D_t data) and is then incident on the LD_2 target. Neutrons from the $d(\vec{p},\vec{n})pp$ reaction pass through a collimator at 9 degrees (laboratory), through a vertical field spin precession magnet, a horizontal field spin precession magnet (off for D_t data), and are incident on an LH_2 target. Recoiling protons are scattered left or right into proton range counters with full track reconstruction and TOF determination. A neutron beam profile monitor and four-branch polarimeter are at the end of the neutron beam line.

2) The deduced ratio D_t/R_t for free np scattering. The experimental values (solid squares) are displayed along with the phase shift predictions of Arndt (solid line), Saclay (broken lines) over two energy regions, and BASQUE (open circles). The phase shift predictions are from reference 13.

3) Phase shifts before and after inclusion of the present data. The values are derived from reference 13 for the energy independent solutions C200, C300, C400, and C500 before (open triangles) and after (solid squares) inclusion of the present data. The most significantly affected phase shifts are displayed: $^1P_1$; $^3S_1$; ϵ_1; $^3D_1$; $^3D_2$; and ϵ_3. These results should be regarded only as a qualitative indication of the impact of this experiment on the phase shifts rather than the result of a full parameter fit to the whole data base.

Table I. Systematic Errors in d_t/r_t.

Energy T_p (MeV)	(A) Foil 'Burn-out' Limit on A_k variation (relative)	d_t/r_t error	(B) Spin precession d_t/r_t error	(C) Additional Components of polarization limit on $a_t P_z$	d_t/r_t error	(D) Beam Motion Change in A_y at LH_2	d_t/r_t error	(G) Energy Slope in d_t/r_t vs. energy	d_t/r_t error	Total d_t/r_t error
223	± 0.9%	± 0.0001	± 0.00006	± 0.0026	± 0.00005	± 0.00026	± 0.000004	- 0.0022	± 0.0033	± 0.0033
324	± 0.5%	± 0.0010	± 0.0008	± 0.0072	± 0.0017	± 0.00039	± 0.00008	- 0.0016	± 0.0024	± 0.0032
425	± 1.0%	± 0.0034	± 0.0014	± 0.0058	± 0.0025	± 0.00042	± 0.0001	- 0.0015	± 0.0023	± 0.0050
492	± 1.1%	± 0.0048	± 0.0018	± 0.0036	± 0.0022	± 0.00078	± 0.0003	- 0.0015	± 0.0023	± 0.0060

Table II. Experimental Results for d_t/r_t and Deduced values for D_t/R_t.

T_p (MeV)	T_n (MeV)	$W_{c.m.}$ (MeV)	θ_n (c.m.) (degrees)	d_t/r_t (Value) ± (stat.) ± (sys.)	Δ-T_n cut-off (MeV)	Additional Error in D_t/R_t due to error in ΔT_n	D_t/R_t
223	223	1986	161.0	0.0144 ± 0.0064 ± 0.0033	31 ± 9	± 0.0004	- 0.0190 ± 0.0095
324	325	2034	160.5	-0.1916 ± 0.0046 ± 0.0032	55 ± 12	± 0.0010	- 0.2328 ± 0.0069
425	425	2080	160.1	-0.3380 ± 0.0045 ± 0.0050	89 ± 13	± 0.0009	- 0.3731 ± 0.0075
492	493	2110	159.8	-0.4391 ± 0.0085 ± 0.0060	101 ± 16	± 0.0024	- 0.4892 ± 0.0119

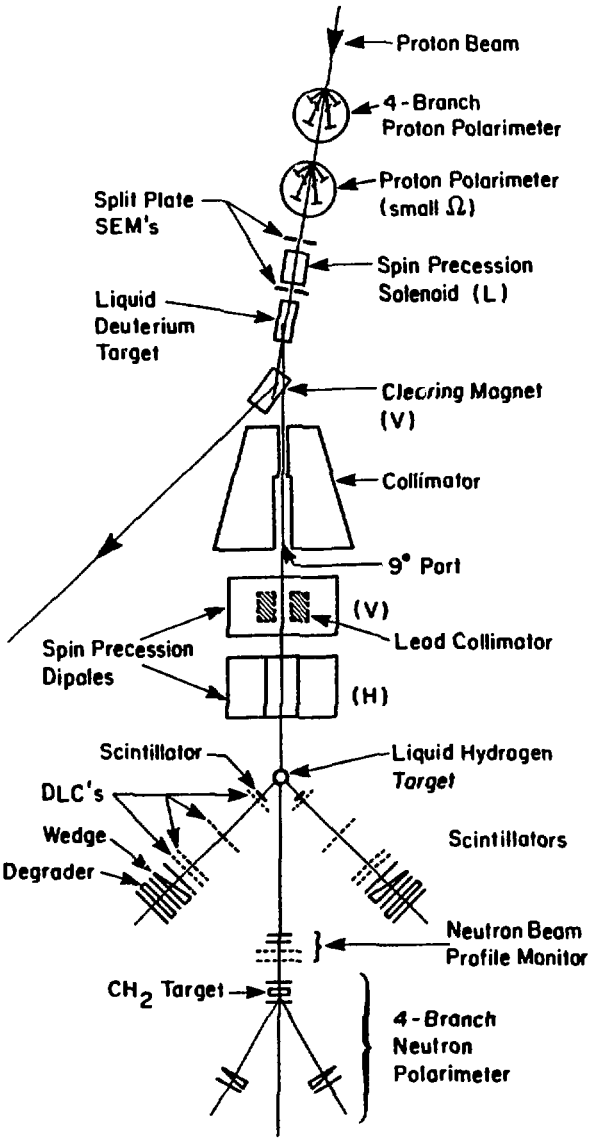
Proton Beam
4-Branch
Proton Polarimeter
Proton Polarimeter
(small Ω)
Split Plate
SEM's
Spin Precession
Solenoid (L)
Liquid
Deuterium
Target
Clearing Magnet
(V)
Collimator
9° Port
(V)
Lead Collimator
Spin Precession
Dipoles
(H)
Scintillator
Liquid Hydrogen
Target
DLC's
Wedge
Degrader
Scintillators
Neutron Beam
Profile Monitor
CH_2 Target
4-Branch
Neutron
Polarimeter

Fig. 1

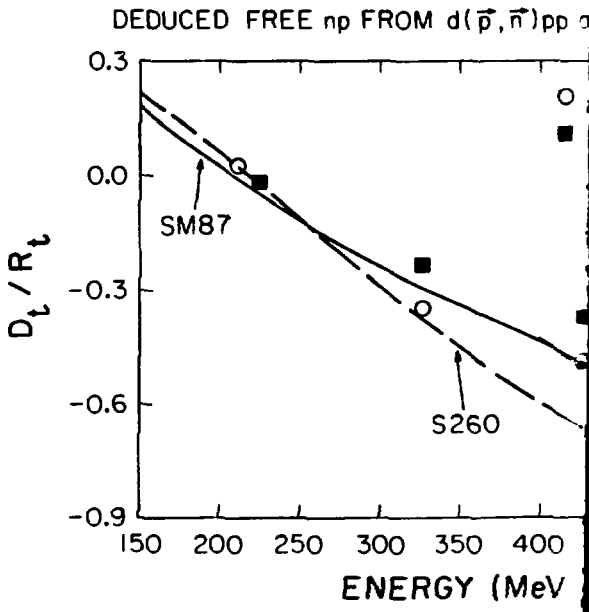
DEDUCED FREE np FROM d(p⃗,n⃗)pp
0.3
0.0
-0.3
-0.6
-0.9
D_t / R_t
SM87
S260
150
200
250
300
350
400
ENERGY (MeV

Fig. 2

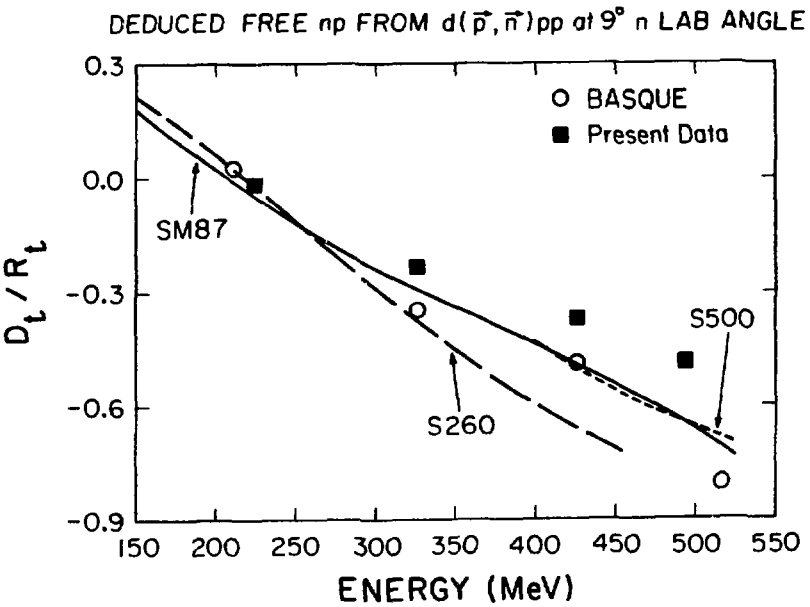
DEDUCED FREE np FROM d(p⃗, n⃗)pp at 9° n LAB ANGLE
BASQUE
Present Data
SM87
S500
S260
D_t / R_t
ENERGY (MeV)

Fig. 2

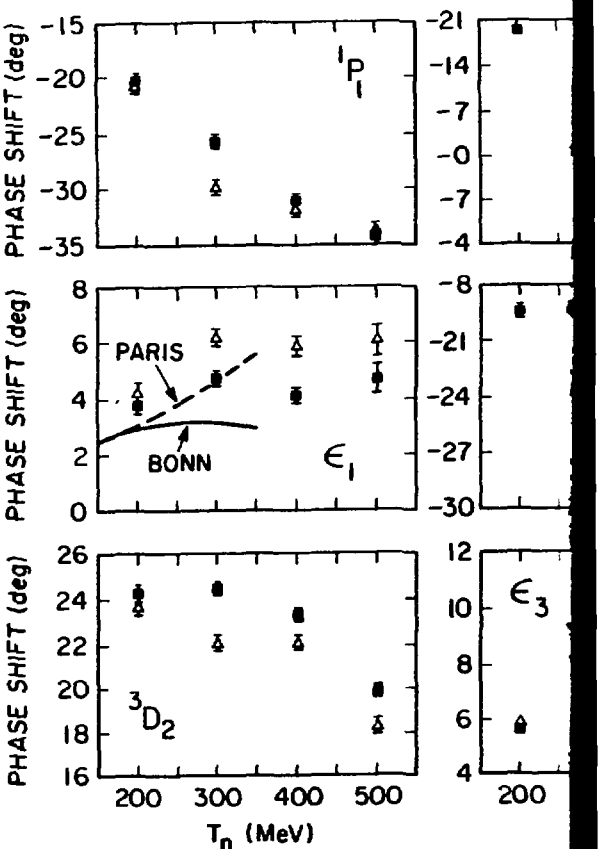
PHASE SHIFT (deg)
$^1P_1$
PARIS
BONN
ϵ_1
$^3D_2$
ϵ_3
T_n (MeV)
Δ-SAID (SM87)
▪-ADDITION OF D_t / R_t DATA

Fig. 3

FROM $d(\vec{p},\vec{n})pp$ at 9° n LAB ANGLE

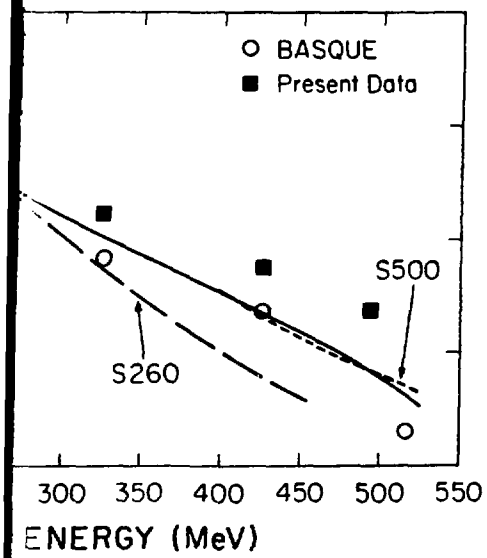

Fig. 2

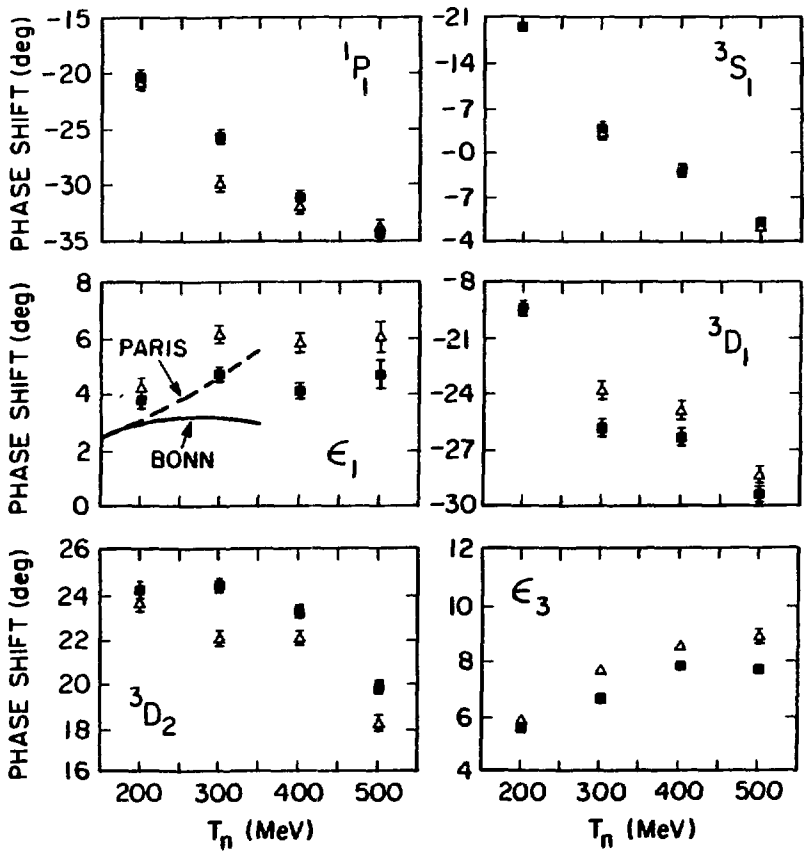

△-SAID (SM87)

■-ADDITION OF D_t/R_t DATA

Fig. 3